Partial Isothermal Sections of the Cu-Rich Corner of the Al-Cu-Zn System at 200 and 240 °C

Article *in* Journal of Phase Equilibria and Diffusion · August 2019

DOI: 10.1007/s11669-019-00746-8

J. Phase Equilib. Diffus.
https://doi.org/10.1007/s11669-019-00746-8

Partial Isothermal Sections of the Cu-Rich Corner of the Al-Cu-Zn System at 200 and 240 °C

J. Ngugi[1,2] · G. O. Rading[1,2] · B. O. Odera[2,3] · B. Ngobe[4] · R. Forbes[5] · L. A. Cornish[2,6]

Submitted: 6 May 2019 / in revised form: 29 June 2019

Abstract Partial isothermal sections of the Cu-rich corner of ternary Al-Cu-Zn system at 200 and 240 °C were plotted up to 55 at.% Cu and 85 at.% Zn based on scanning electron microscopy, energy-dispersive x-ray spectroscopy and x-ray diffractometry analyses of ten ternary alloys. Seven phases were observed at both isothermal temperatures, and no new ternary phases were found. The results were compared with previously published works, and the γ-phase was confirmed to exist as two phases: γ Cu_9Al_4 and γ Cu_5Zn_8.

Keywords alloys · binary system · isothermal section · phase diagram · phase equilibria · ternary phase

1 Introduction

The Al-Cu-Zn system is well used because the alloys have demonstrated many useful properties. Currently, Al-Cu-Zn alloys with the β-phase are commercially used as shape memory alloys (SMAs) since they undergo reversible martensitic transformations which impart shape memory behaviour.[1,2] Their use as SMAs is more economical than the use of Ni-Ti alloys.[3] Al-Cu-Zn alloys are also used as catalysts[4,5] and as matrices for particle-reinforced composites.[6] Al-Cu-Zn alloys with microstructures comprising ε, (ηZn) and (αAl) have been targeted as potential candidates to replace the brittle and high-cost Bi- and Ni-based solders in temperature applications up to 350 °C.[7]

2 Brief Overview of the Binary Systems

The constituent binary systems of the Al-Cu-Zn system are Al-Cu, Cu-Zn and Al-Zn systems.

The Al-Cu is a well-researched system with more emphasis on the Al-rich side due to the importance of Al alloys in the transport industry. Murray[8] published the first assessment in 1985. Other studies have been done by Liu et al.,[9] Riani[10] and Ponweiser et al.[11] Generally, there is a qualitative agreement between researchers on the phase equilibria of the system. The system has two eutectic reactions (at 17.1 and 83.0 at.% Cu) and 12 intermetallic compounds, seven of which are stable at high temperatures.[8]

The Cu-Zn system is also well established, and there are no major disagreements between the works reviewed by

✉ J. Ngugi
johnson.ngugi@students.uonbi.ac.ke

1 Department of Mechanical and Manufacturing Engineering, University of Nairobi, Nairobi, Kenya

2 African Materials Science and Engineering Network (AMSEN) (A Carnegie-RISE Network), University of the Witwatersrand, Johannesburg, South Africa

3 School of Mechanical and Process Engineering, Technical University of Kenya, Nairobi, Kenya

4 Advanced Materials Division, Mintek, Randburg, South Africa

5 Molecular Sciences Institute, School of Chemistry, University of the Witwatersrand, Johannesburg, South Africa

6 DST-NRF Centre of Excellence in Strong Materials and School of Chemical and Metallurgical Engineering, University of the Witwatersrand, Johannesburg, South Africa

Published online: 17 August 2019

Raynor,[12] Hansen and Anderko,[13] Massalski et al.,[14] Miodownik[15] and Predel.[16] The system forms peritectic reactions at 902, 834, 700, 598 and 425 °C and a eutectoid reaction at 560 °C.[15]

Two different phase diagrams have been published for the Al-Zn system. One version of the phase diagram was produced by Presnyakov et al.[17] in 1963 and later modified by Goldak and Parr,[18] while the other was reported by Murray[19] in 1985. Three main features present in the diagram modified by Goldak and Parr[18] are missing in Murray's[19] diagram: peritectic transformation at 443 °C, second monotectoid reaction at 340 °C, and intermetallic β-phase between 49.77 and 63.13 at.% Zn at 340 °C (with its narrow two-phase (α′ + β) region at 51.48 at.% Zn at 340 °C). Since the current study was on much lower temperatures where there is no significant disparity between the two diagrams,[18,19] Murray's[19] diagram was accepted.

3 Al-Cu-Zn System

The phase equilibria of the Al-Cu-Zn system have received considerable attention since the turn of the twentieth century as reviewed by Liang and Chang.[20] The liquidus surface was first given by Köster[21] and then later modified by Arndt and Moeller.[22] Calphad thermodynamic descriptions have been developed by Liang and Chang,[20] Miettinen[23] and Liang and Schmid-Fetzer.[24] The τ-phase forms at about 740 °C through a univariant peritectic reaction between liquid and the binary Al-Cu phase ε_2.[3] The τ′ phase appears at the Al-rich end of the homogeneity range of τ at between 600 °C and 500 °C and exists as a stable phase at 300 °C.[3,25] Chen et al.[26] showed that the τ′ phase is stable at room temperature. Villegas-Cardenas et al.[27] investigated the effect of small additions of copper on hardness in Zn-rich aluminium alloys and observed a positive correlation between them, which they attributed to the formation of copper-containing θ and τ′ phases.

Ghosh et al.[3] reviewed all isothermal sections published until 2002. The sections by Köster and Moeller[28] at 200 °C and Gebhardt[29] at 240 °C, plotted in mass% as shown in Fig. 1 and 2, were incomplete at their Cu-rich corners and formed the basis of this study. There are also differences regarding the nature of the γ-phase as highlighted by Liang and Schmid-Fetzer.[24] Bauer and Hansen[30] proposed that γ forms a continuous phase field from the Al-Cu binary edge to the Cu-Zn edge, which was accepted subsequently.[21,22,31,32] However, Kandaurov et al.[33] and Ashrimbetov et al.[34] later observed a two-phase region between γ Cu_9Al_4 and γ Cu_5Zn_8.

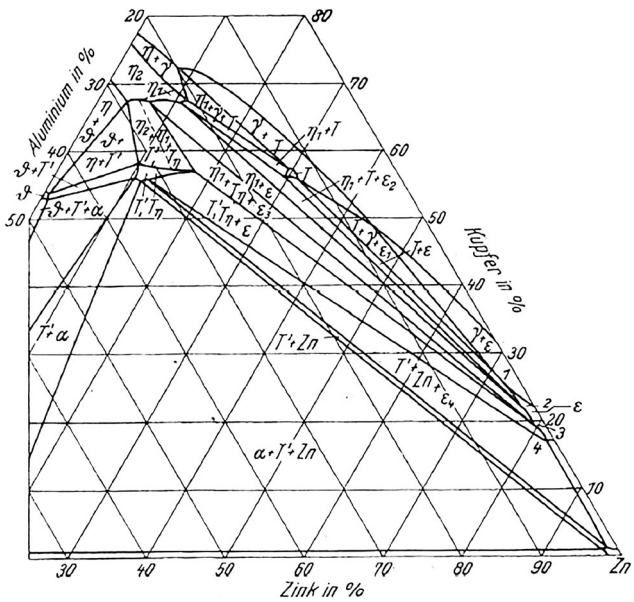

Fig. 1 Isothermal section in mass% of Al-Cu-Zn system at 200 °C by Köster and Moeller[28] where α = (αAl), γ = γ Cu_9Al_4 and γ Cu_5Zn_8, η_2 = η_2 CuAl, ζ = ζ_2 $Cu_{11}Al_9$, ε = ε $CuZn_4$, T = τ $Cu_5Zn_2Al_3$ and $T'T_\eta$ = τ′ Cu_3ZnAl_4

4 Experimental Procedure

Ten ternary alloy compositions were selected in the multiphase regions around the Cu-rich corner using the isothermal section at 240 °C reviewed by Ghosh et al.[3] Pure aluminium (99.9 at.%), copper (99.9 at.%) and zinc (99.9 at.%) pellets were used for sample preparation. Initial melting in an arc furnace under an argon atmosphere was unsuccessful as Zn vaporised before Cu could melt. Only two alloys with low Zn content were successfully prepared in the second attempt in a hot platinum induction furnace under the same inert conditions. The other eight alloys with higher Zn content were prepared in a graphite induction furnace in stages. Copper was melted first and then Al added to lower the liquidus below the boiling point of Zn. Zn was finally added and a ceramic rod used to stir to facilitate mixing.

An SBT (South Bay Technology) low-speed diamond wheel saw (Model 650) was used to cut each alloy in half. Two sets of samples were separately sealed in vacuum glass ampoules and homogenised at 370 °C for 10 days in an Elsklo LN 2 muffle furnace. One set was annealed at 200 °C and the other set annealed at 240 °C for 4 weeks. All samples were ground on successively finer SiC papers of grit sizes ranging from #300 to #800 and then polished using diamond paste with sizes from 6 to ¼ μm. A Leo 1525 Field Emission and FIB Crossbeam 540 scanning electron microscopes (SEMs) coupled with energy-dispersive x-ray spectrometers (EDS) were used to characterise

the microstructures of the alloys, and the BSE mode was mainly used. The XRD data were obtained using a PANalytical Empyrean XRD system with Cu $K\alpha$ radiation operated at a voltage of 45 kV and a current of 40 mA, and the data were compared to the 2017 ICDD database. Sample A5 was also subjected to Rietveld analysis, analysing the sample from both sides.

5 Results and Discussion

The targeted versus the analysed compositions of the ternary alloys are shown in Table 1. The targeted compositions were not achieved for all samples, and this was attributed to Zn loss during casting. Phases were distinguished from each other on the basis of contrast in BSE mode, EDS compositions and from XRD. All of the peaks were matched with the database, showing that there were no new phases. EDS phase compositions are given in Table 2.

Seven phases were identified from BSE images at both 200 and 240 °C: binary (αCu), γ Cu_9Al_4, η_2 CuAl, γ Cu_5Zn_8, ζ_2 $Cu_{11}Al_9$ and ε $CuZn_4$ phases, and the ternary τ $Cu_5Zn_2Al_3$ and τ′ Cu_3ZnAl_4 phases. No previously unreported ternary phases were observed by XRD because all the peaks were matched. However, traces of β Cu-Zn were observed in the XRD pattern of Sample A8, showing the sample was not single phase. Although α_2 Cu_4Al and δ Cu_8Al_5 phases might have been expected in the region studied, they were not observed in any alloy.

BSE micrographs of Samples A1, A5, A6, A7 and A8 annealed at both 200 and 240 °C and their corresponding XRD patterns are given in Fig. 3, 4, 5, 6, 7, 8, 9, 10, 11 and 12. EDS sample analyses at 200 °C and 240 °C were plotted in at.% and are shown Fig. 13 and 14 in at.%, respectively.

In an attempt to discern whether Sample A5 has Cu_5Zn_8 or Cu_9Al_4, Rietveld analysis was used on both sides of the sample. The data in the phase identification plot (Fig. 15) showed several differences in the intensity of the major

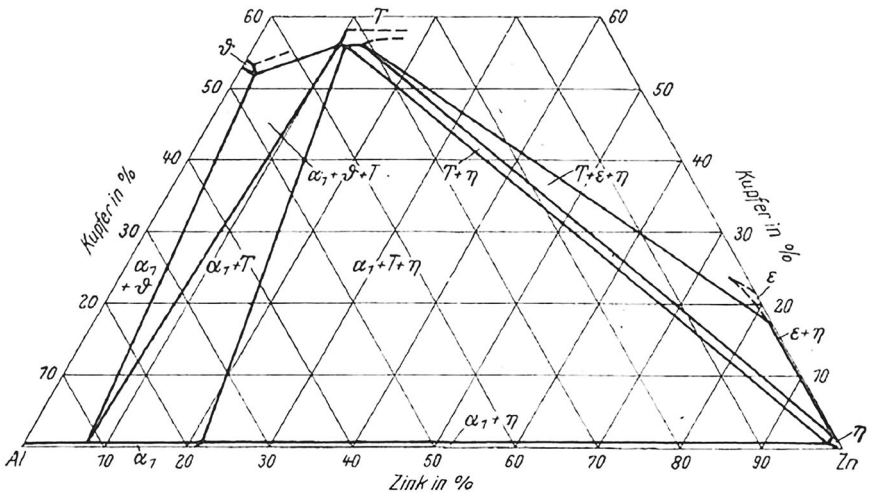

Fig. 2 Isothermal section in mass% of Al-Cu-Zn system at 240 °C reviewed by Gebhardt[29] where α_1 = (αAl), ε = ε $CuZn_4$, η = (ηZn), ζ = ζ_2 $Cu_{11}Al_9$ and T = τ $Cu_5Zn_2Al_3$

Table 1 Targeted vs. analysed composition of ternary alloy samples

Sample	Target composition, at.%			Analysed composition, at.%		
	Al	Cu	Zn	Al	Cu	Zn
A1	15.8	80.0	4.2	14.9 ± 0.2	68.6 ± 0.2	16.5 ± 0.3
A2	20.0	62.1	17.9	16.0 ± 0.2	78.9 ± 0.2	5.1 ± 0.3
A3	31.6	62.1	6.3	27.8 ± 0.3	55.5 ± 0.2	16.6 ± 0.3
A4	3.7	65.8	30.5	19.0 ± 0.2	74.5 ± 0.3	6.5 ± 0.4
A5	20.0	62.1	17.9	14.3 ± 0.3	42.2 ± 0.3	43.5 ± 0.5
A6	14.7	50.5	34.7	13.0 ± 0.1	36.9 ± 0.2	50.2 ± 0.1
A7	44.0	43.0	13.0	41.9 ± 0.4	42.2 ± 0.6	15.9 ± 0.3
A8	30.0	45.0	25.0	25.8 ± 0.5	38.9 ± 0.3	35.3 ± 0.8
A9	18.0	28.0	54.0	21.0 ± 1.6	22.3 ± 0.6	56.7 ± 2.0
A10	6.0	20.0	74.0	10.9 ± 1.6	17.4 ± 1.5	71.8 ± 1.6

Table 2 EDS compositions of the overalls and phases: Cu:Zn:Al (at.%), with small areas shown in italics, present = phase too small to analyse, eutectic = phase was part of a eutectic, eutectoid = phase was part of a eutectoid

Sample	Temperature, °C	Observed phases	Overall analysis	(αCu)	γ Cu_5Zn_8	ε $CuZn_4$	γ Cu_9Al_4	ζ_2 $Cu_{11}Al_9$	η_2 CuAl	τ $Cu_5Zn_2Al_3$	τ′ Al_3ZnAl_4
A1	200	(αCu)	68.6 ± 0.2	71.8 ± 0.4	…	…	Present, eutectic	…	…	…	…
		γ Cu_9Al_4	16.5 ± 0.3	16.7 ± 0.5							
			14.9 ± 0.2	11.5 ± 0.1							
	240	(αCu)	68.6 ± 0.2	71.7 ± 0.3			Present, eutectic				
		γ Cu_9Al_4	16.7 ± 0.1	16.8 ± 0.4							
			14.7 ± 0.1	11.5 ± 0.2							
A2	200	(αCu)	79.1 ± 0.2	79.1 ± 0.2	…	…	Present, eutectic	…		…	…
		γ Cu_9Al_4	5.1 ± 0.3	5.4 ± 0.1							
			15.8 ± 0.2	15.5 ± 0.2							
	240	(αCu)	78.9 ± 0.1	79.1 ± 0.2	…	…	…	…	…	…	…
			5.1 ± 0.1	5.1 ± 0.2							
			16.0 ± 0.1	15.8 ± 0.2							
A3	200	γ Cu_9Al_4	55.6 ± 0.2	…	…	…	58.2 ± 0.1	…	…	48.4 ± 0.6	…
		τ $Cu_5Zn_2Al_3$	16.6 ± 0.3				13.3 ± 0.1			26.8 ± 1.0	
			27.8 ± 0.3				28.5 ± 0.1			24.8 ± 0.4	
	240	γ Cu_9Al_4	55.0 ± 0.4	…	…	…	57.6 ± 0.2	…	…	47.8 ± 0.1	…
		τ $Cu_5Zn_2Al_3$	16.9 ± 0.5				13.4 ± 0.2			27.0 ± 0.1	
			28.1 ± 0.2				29.0 ± 0.2			25.2 ± 0.2	
A4	200	(αCu)	75.3 ± 0.3	77.5 ± 0.3	…	…	72.8 ± 0.4	…	…	…	…
		γ Cu_9Al_4	6.1 ± 0.4	6.1 ± 0.2			6.3 ± 0.2				
			18.6 ± 0.2	16.4 ± 0.2			20.9 ± 0.5				
	240	(αCu)	74.5 ± 0.4	76.7 ± 0.4	…	…	*68.7 ± 0.6*	…	…	…	…
		γ Cu_9Al_4	6.5 ± 0.2	6.0 ± 0.1			*5.5 ± 0.3*				
			19.0 ± 0.3	17.3 ± 0.4			*25.8 ± 0.7*, eutectic				
A5	200	γ Cu_5Zn_8	42.2 ± 0.3	…	37.4 ± 0.1	…	57.2 ± 0.4	…	…	48.0 ± 0.1	…
		γ Cu_9Al_4	43.5 ± 0.5		56.9 ± 0.2		16.0 ± 0.9			28.4 ± 0.1	
		τ $Cu_5Zn_2Al_3$	14.3 ± 0.3		5.7 ± 0.2		26.8 ± 0.6			23.6 ± 0.1	
	240	γ Cu_5Zn_8	42.9 ± 0.4	…	39.4 ± 0.1	…	55.4 ± 0.3	…	…	48.3 ± 0.1	…
		γ Cu_9Al_4	42.6 ± 0.8		52.8 ± 0.1		20.3 ± 0.5			28.5 ± 0.1	
		τ $Cu_5Zn_2Al_3$	14.5 ± 0.4		7.8 ± 0.1		24.3 ± 0.3			23.2 ± 0.2	
A6	200	γ Cu_5Zn_8	36.9 ± 0.2	…	40.9 ± 0.3		…	…	…	*45.3 ± 0.6*	…
		ε $CuZn_4$	50.1 ± 0.1		48.8 ± 0.5					*32.7 ± 1.0*	
		τ $Cu_5Zn_2Al_3$	13.0 ± 0.1		10.3 ± 0.3	Eutectoid				*22.0 ± 0.5*	
	240	γ Cu_5Zn_8	36.8 ± 0.9	…	37.1 ± 0.2	27.1 ± 0.2	…	…	…	47.9 ± 0.3	…
		ε $CuZn_4$	50.0 ± 1.4		56.8 ± 0.4	67.5 ± 0.3				27.8 ± 0.2	

Table 2 continued

Sample	Temperature, °C	Observed phases	Overall analysis	(αCu)	γ Cu_5Zn_8	ε $CuZn_4$	γ Cu_9Al_4	ζ_2 $Cu_{11}Al_9$	η_2 CuAl	τ $Cu_5Zn_2Al_3$	τ′ Al_3ZnAl_4
		τ $Cu_5Zn_2Al_3$	13.2 ± 0.6		6.1 ± 0.4	5.4 ± 0.2				24.3 ± 0.3	
A7	200	ε $CuZn_4$	42.2 ± 0.6	…	…	21.1 ± 0.2	…	…	45.3 ± 0.1	*40.5 ± 0.2*	…
		η_2 CuAl	15.9 ± 0.3			76.0 ± 0.3			11.2 ± 0.1	*13.2 ± 0.4*	
		τ $Cu_5Zn_2Al_3$	41.9 ± 0.4			2.9 ± 0.2			43.5 ± 0.1	*46.3 ± 0.3*	
	240	ε $CuZn_4$	42.3 ± 0.5	…	…	*23.0 ± 0.6*	…	43.4 ± 0.2	43.5 ± 0.3	…	…
		ζ_2 $Cu_{11}Al_9$	16.1 ± 0.3			*72.4 ± 0.9*		15.4 ± 0.2	15.4 ± 0.2		
		η_2 CuAl	41.6 ± 0.4			*4.6 ± 0.4*		41.2 ± 0.2	41.1 ± 0.3		
A8	200	ε $CuZn_4$	38.9 ± 0.3	…	…	24.7 ± 0.2	…	49.0 ± 0.3	…	47.6 ± 0.2	…
		ζ_2 $Cu_{11}Al_9$	35.3 ± 0.8			71.4 ± 0.2		13.3 ± 0.4		25.9 ± 0.1	
		τ $Cu_5Zn_2Al_3$	25.8 ± 0.5			3.9 ± 0.2		37.7 ± 0.3		26.6 ± 0.2	
	240	ε $CuZn_4$	37.7 ± 0.5	…	…	26.0 ± 0.4	…	48.1 ± 0.2	…	44.9 ± 1.0	…
		ζ_2 $Cu_{11}Al_9$	36.6 ± 0.8			67.7 ± 0.5		13.0 ± 0.6		26.8 ± 1.3	
		τ $Cu_5Zn_2Al_3$	25.6 ± 0.6			6.3 ± 0.4		38.9 ± 0.4		28.3 ± 0.4	
A9	200	ε $CuZn_4$	2.3 ± 0.6	…	…	18.8 ± 0.1	…	…	…	…	38.8 ± 0.7
		τ′ Al_3ZnAl_4	56.7 ± 2.0			79.4 ± 0.1					8.7 ± 0.4
			21.0 ± 1.6			1.8 ± 0.1					52.5 ± 0.5
	240	ε $CuZn_4$	21.6 ± 0.7	…	…	17.6 ± 0.2	…	…	…	…	39.1 ± 0.2
		τ′ Al_3ZnAl_4	57.4 ± 1.3			80.5 ± 0.2					7.7 ± 0.8
			21.0 ± 1.0			1.9 ± 0.1					53.2 ± 1.0
A10	200	ε $CuZn_4$	17.4 ± 1.5	…	…	20.4 ± 0.2	…	…	…	…	*38.4 ± 0.8*
		τ′ Al_3ZnAl_4	71.7 ± 1.6			77.1 ± 0.2					*9.1 ± 1.2*
			10.9 ± 1.6			2.5 ± 0.1					*52.5 ± 0.7*
	240	ε $CuZn_4$	19.3 ± 0.3	…	…	20.6 ± 0.2	…	…	…	…	*40.0 ± 0.5*
		τ′ Al_3ZnAl_4	69.7 ± 0.4			76.2 ± 0.2					*10.0 ± 0.1*
			10.9 ± 0.4			3.2 ± 0.1					*50.0 ± 0.5*

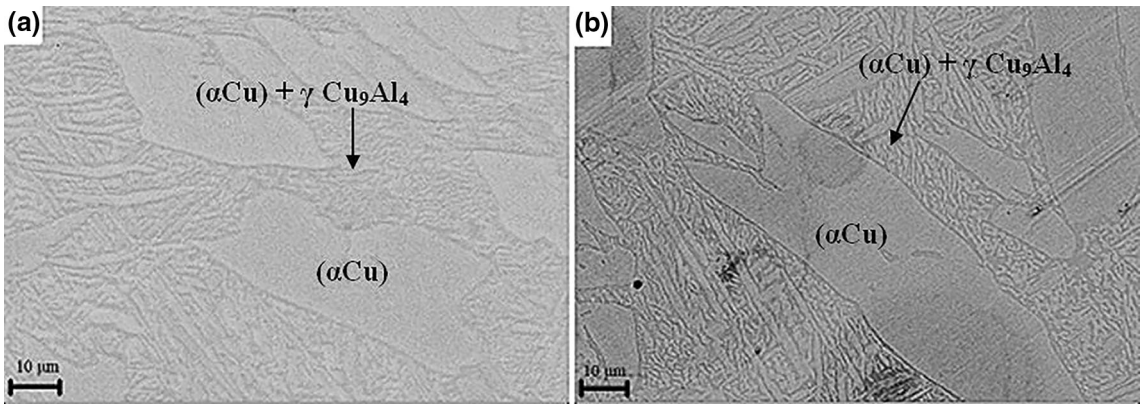

Fig. 3 BSE images of Sample A1 with nominal composition $Cu_{68.6}Zn_{16.7}Al_{14.7}$ (at.%): (a) annealed at 200 °C, (b) annealed at 240 °C

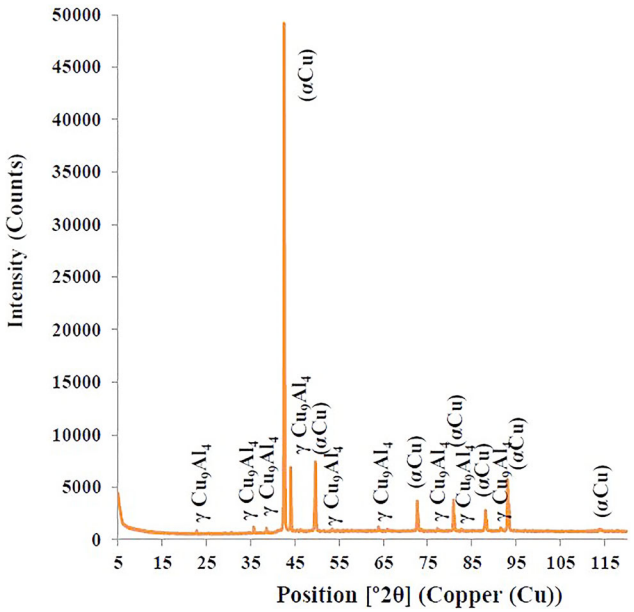

Fig. 4 XRD pattern of Sample A1 with nominal composition $Cu_{68.6}Zn_{16.7}Al_{14.7}$ (at.%) annealed at 200 °C

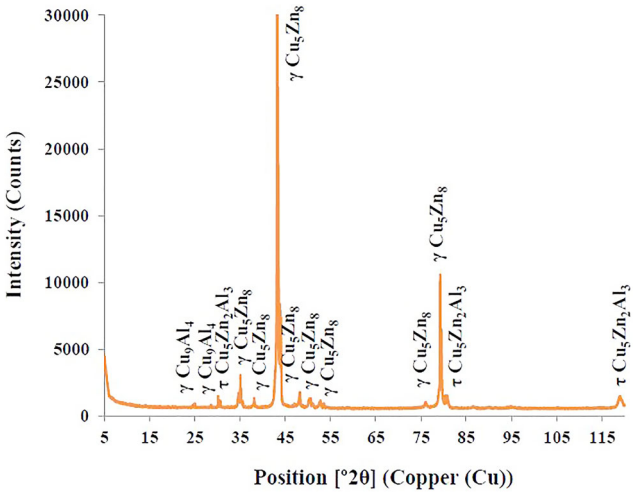

Fig. 6 XRD pattern of Sample A5 with nominal composition $Cu_{42.2}Zn_{43.5}Al_{14.3}$ (at.%) annealed at 200 °C

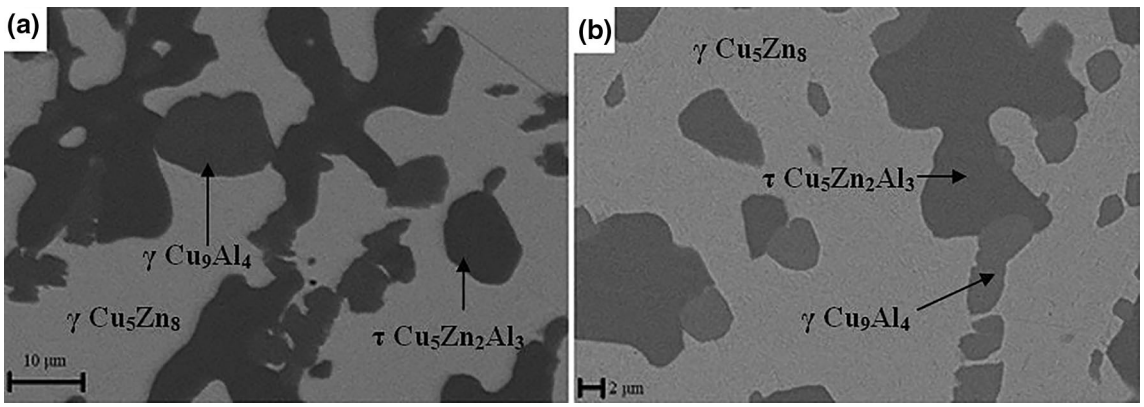

Fig. 5 BSE images of Sample A5 with nominal composition $Cu_{42.2}Zn_{43.5}Al_{14.3}$ (at.%): (a) annealed at 200 °C, (b) annealed at 240 °C

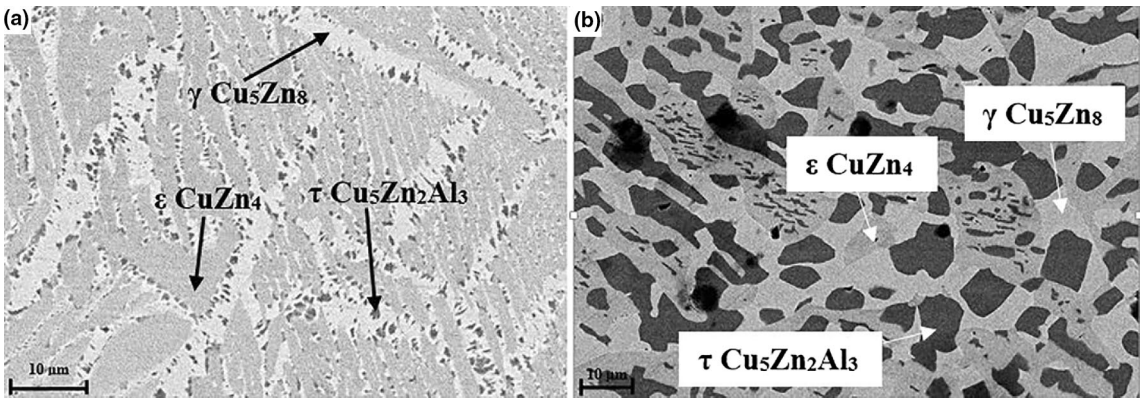

Fig. 7 BSE images of Sample A6 with nominal composition $Al_{13.2}Cu_{36.8}Zn_{50}$ (at.%): (a) annealed at 200 °C, (b) annealed at 240 °C

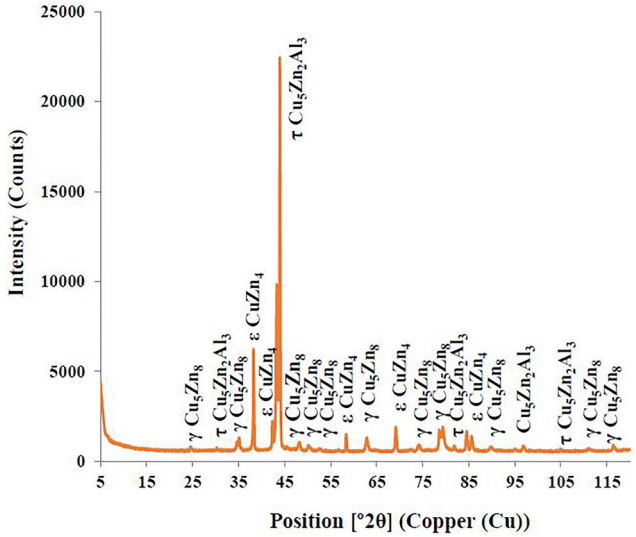

Fig. 8 XRD pattern of Sample A6 with nominal composition $Al_{13.2}Cu_{36.8}Zn_{50}$ (at.%) annealed at 200 °C

reflections observed in each sample, which was likely due to sample texturing. Phase identification showed that the sample likely comprised the Cu_5Zn_8 and Cu_9Al_4 phases, and the proportions in Fig. 16 ($\sim$ 69% for Cu_5Zn_8 and $\sim$ 31% for Cu_9Al_4) agree with the positions (i.e., using the lever rule) in Fig. 13 and 14. However, Rietveld refinement of the data could not produce a satisfactory fit with which to obtain quantitative phase data (Fig. 16). This is due to the database entries of the Cu_5Zn_8 and Cu_9Al_4 phases being either incomplete or different from those observed in Sample A5. Partial structural refinement using analogous structure types also yielded poor results. Furthermore, the Rietveld refinement of the data collected on each side of the sample produced different (due to sample texturing), albeit meaningless, quantitative data. Further study using more sensitive techniques such as XAFS or PDF would be required in order to decisively partition the contributions arising from each individual phase and would allow for more accurate phase quantification. However, this is beyond the scope of this project, and the techniques were not accessible at the time of the project.

Sample 1A had (αCu) and a eutectic of (αCu) + γ Cu_9Al_4 at both annealing temperatures as illustrated in Fig. 3(a) and (b). Moreover, the (αCu) boundary at 240 °C was similar to that at 200 °C.

The debate on the nature of the γ-phase was recognised by Liang and Schmid-Fetzer[24] who traced it to Bauer and

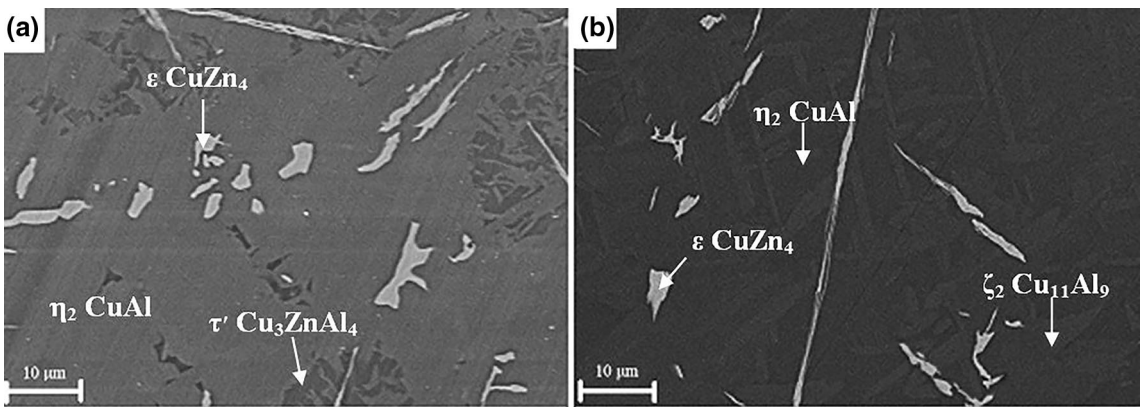

Fig. 9 BSE images of Sample A7 with nominal composition $Al_{41.6}Cu_{42.3}Zn_{16.1}$ (at.%): (a) annealed at 200 °C, (b) annealed at 240 °C

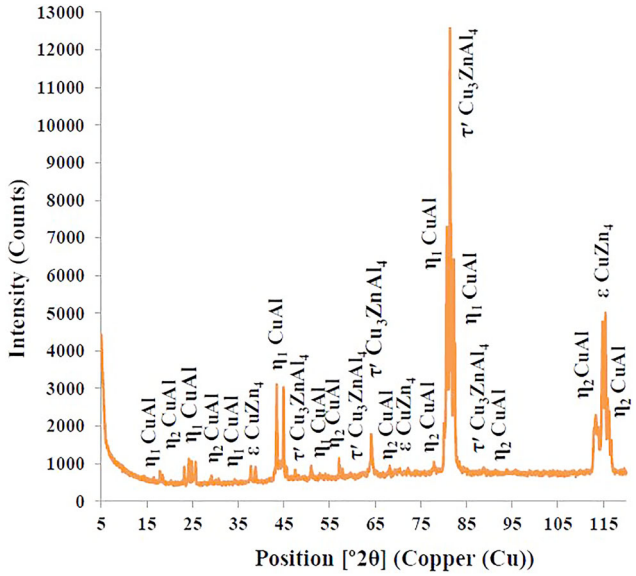

Fig. 10 XRD pattern of Sample A7 with nominal composition $Al_{41.6}Cu_{42.3}Zn_{16.1}$ (at.%) annealed at 200 °C

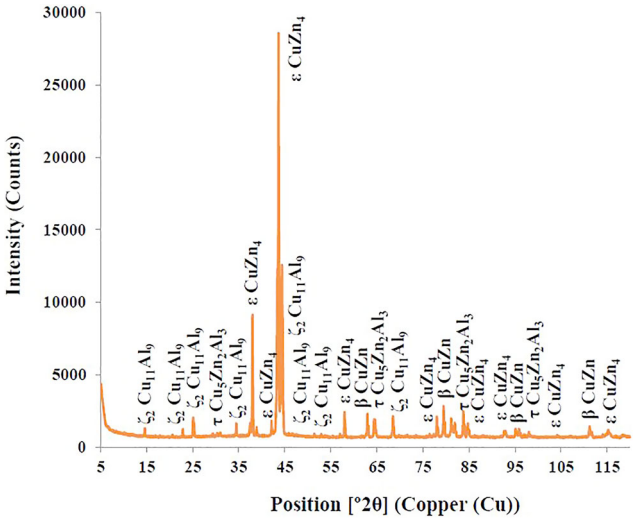

Fig. 12 XRD pattern of Sample A8 with nominal composition $Al_{25.6}Cu_{37.8}Zn_{36.6}$ (at.%) annealed at 200 °C

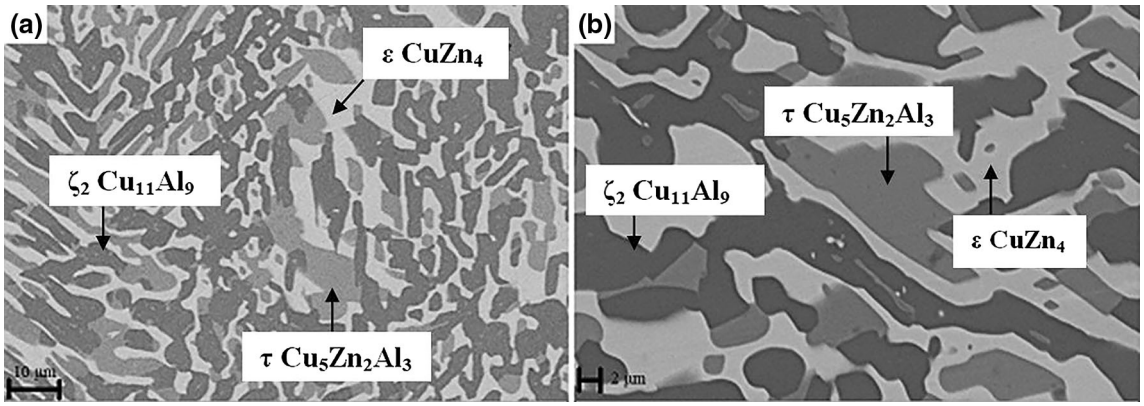

Fig. 11 BSE images of Sample A8 with nominal composition $Al_{25.6}Cu_{37.8}Zn_{36.6}$ (at.%): (a) annealed at 200 °C, (b) annealed at 240 °C

Hansen[30] in 1932. Bauer and Hansen[30] suggested a continuous single-solid phase field for γ from the Al-Cu binary edge to the Cu-Zn edge, even though their work ended at the Cu-rich boundary of γ. This was accepted by several researchers,[21,22,31,32] until Kandaurov et al.[33] (in 1972), and Ashrimbetov et al.[34] (in 1973) observed a two-phase region between the Al-Cu-side γ and CuZn-side γ. In 1998, Liang and Chang[20] modelled a continuous ternary γ-phase in their calculated isothermal sections at 600 and 700 °C, because they based their thermodynamic model on the experimental works of Arndt and Moeller[22] and Köster and Moeller[32] which both reported a continuous γ-phase. The current study confirmed that γ Cu_9Al_4 and γ Cu_5Zn_8 are not the same phase since three phases: γ Cu_9Al_4, τ $Cu_5Zn_2Al_3$ and γ Cu_5Zn_8, were observed in Sample A5 at 200 and 240 °C as shown in Fig. 5. There was poor contrast between γ Cu_9Al_4 and τ $Cu_5Zn_2Al_3$ in Fig. 5(a).

Sample A6, shown in Fig. 7, had τ $Cu_5Zn_2Al_3$, ε $CuZn_4$ and γ Cu_5Zn_8 at both 200 and 240 °C. The three phases may have resulted from a eutectoid decomposition of δ ($\delta \leftrightarrow \tau + \varepsilon + \gamma$) that occurs at 480 °C.[3] However, the sample was coarser at 240 °C, which may be explained by the fact that diffusion increases with temperature. The ε $CuZn_4$ phase appeared to be disappearing at 240 °C, because its proportions were smaller at 240 °C than at 200 °C [for Samples A6 (Fig. 7)], A7 (Fig. 9), and possibly for Sample A8 (Fig. 11). However, the phase field apparently extended at 240 °C (Fig. 14) compared to 200 °C (Fig. 13).

Köster and Moeller[28] reported a solubility range of Cu in τ $Cu_5Zn_2Al_3$ of between 56 wt.% (48.3 at.%) and 58 wt.% (50.3 at.%) at 200 °C. However, the solubility range of Cu in τ $Cu_5Zn_2Al_3$ observed in the current study at 200 °C was between 45.3 ± 0.6 and 48.0 ± 0.1 at.% Cu.

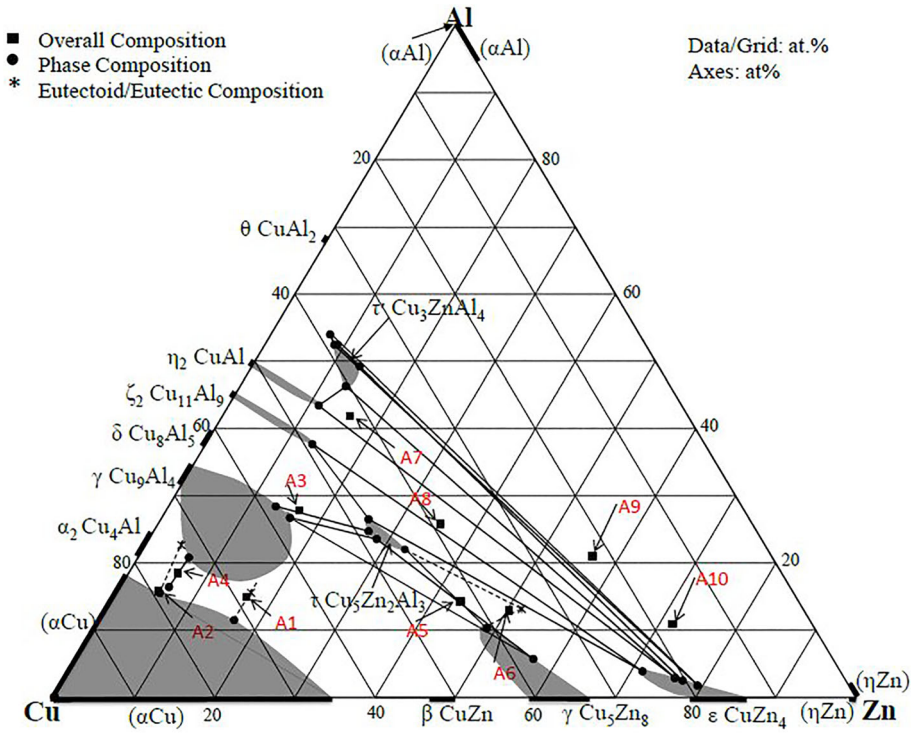

Fig. 13 Analyses of samples annealed at 200 °C (at.%)

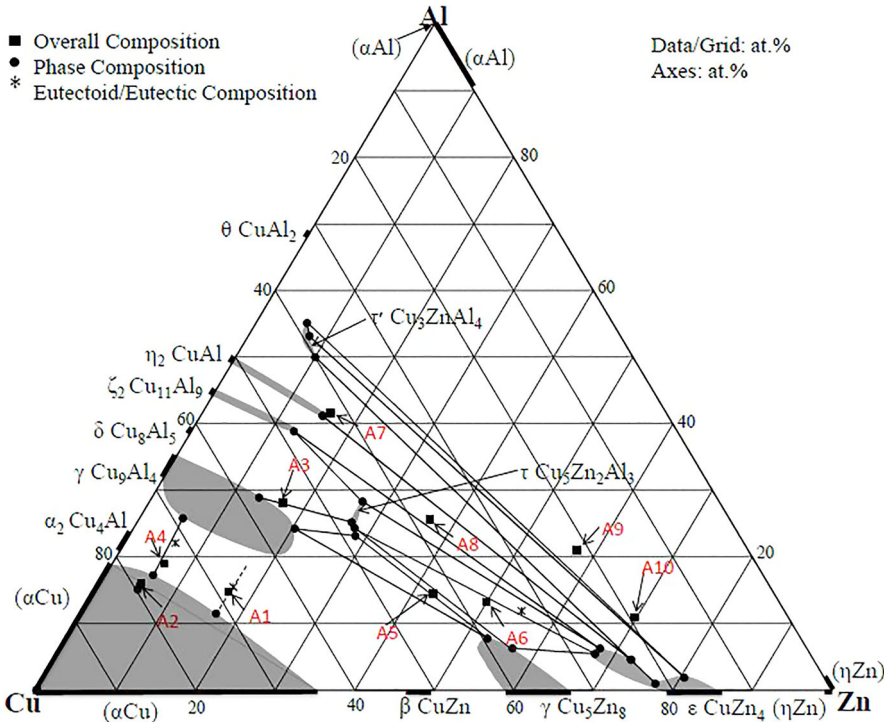

Fig. 14 Analyses of samples annealed at 240 °C (at.%)

The solubility range of Cu in γ Cu_9Al_4 decreased slightly from between 57.2 ± 0.4 and 72.8 ± 0.4 at.% Cu at 200 °C to between 55.4 ± 0.3 and 68.7 ± 0.6 at.% Cu at 240 °C. The τ $Cu_5Zn_2Al_3$ phase had less Zn (28.5 ± 0.1 at.%) at 240 °C than at 200 °C (32.7 ± 1.0 at.%).

The τ′ Cu_3ZnAl_4 phase was present in Sample A7 at 200 °C but was replaced by ζ_2 $Cu_{11}Al_9$ at 240 °C. It showed a solubility range of between 7.4 ± 0.2 at.% Zn and 13.5 ± 2 at.% Zn at 200 °C. This differed slightly with the range reported by Köster and Moeller[28] of

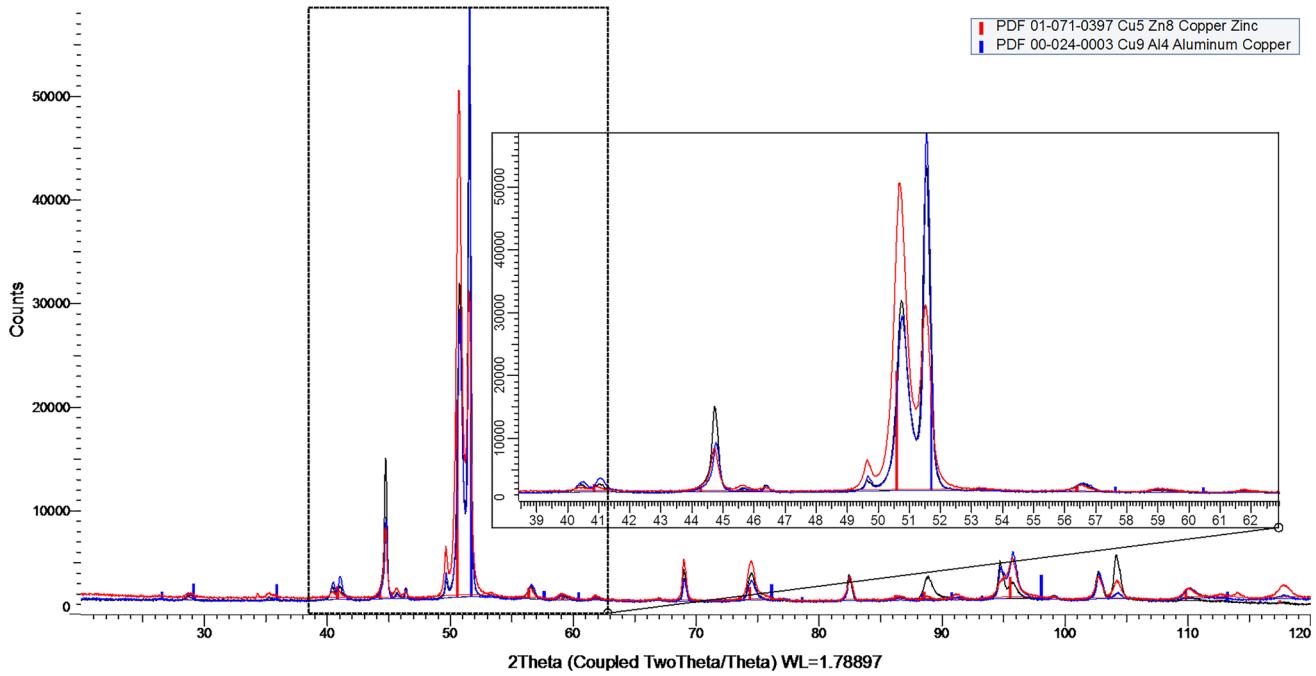

Fig. 15 Comparison of the XRD pattern of Sample A5 with the responses for Cu_9Al_4 and Cu_5Zn_8

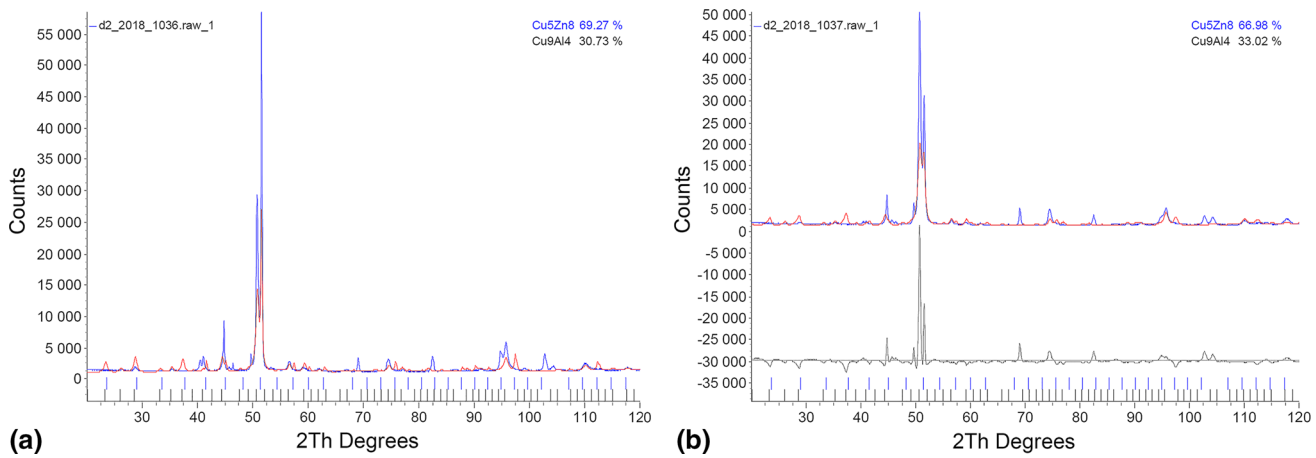

Fig. 16 Comparison of the different sides of Sample A5, showing slight differences in the peaks identified for Cu_9Al_4 and Cu_5Zn_8: (a) first side and (b) second side with Rietveld analysis

between 10 wt.% (6.8 at.%) Zn and 18 wt.% (13.1 at.%) Zn. Although Gebhardt[29] did not assess the entire composition range of τ′ Cu_3ZnAl_4, his assessment showed it has a minimum Cu composition of 55.3 wt.% (38.3 at.%), which is in agreement with the current work (38.4 ± 0.3 at.%). The τ′ Cu_3ZnAl_4 phase has a slightly smaller phase field at 240 °C of between 6.4 ± 0.6 at.% and 10.0 at.% Zn from between 7.4 ± 0.2 and 13.5 at.% Zn at 200 °C.

There was no significant difference between the two microstructures (Fig. 11) of Sample A8. Both had τ $Cu_5Zn_2Al_3$, η_2 CuAl and ε$CuZn_4$ with occasional ε $CuZn_4$ precipitates in the τ $Cu_5Zn_2Al_3$ and η_2 CuAl phases. Even though the high-temperature η_1 CuAl phase does not exist below 560 °C,[8] it was observed in the XRD pattern of Sample A7 in Fig. 10.

According to Fig. 13, the binary ε $CuZn_4$ extended to about 3.9 ± 0.2 at.% Al at 200 °C. This differed slightly with Köster and Moeller's[28] diagram in Fig. 1, which shows the solubility limit of Al in ε $CuZn_4$ at about 3.5 at.%. The extent of ε $CuZn_4$ increased to 6.3 ± 0.4 at.% Al at 240 °C.

However, the samples were not quenched as quickly as they could have been, and some were possibly on the edge of the hot zone of the furnace and could have been annealed at a slightly lower temperature. Additionally,

annealing the samples for 4 weeks may not have been enough to reach thermodynamic equilibrium, and the texturing observed in the XRD patterns is evidence of this, because the preferred orientation of casting should have been removed. If so, this may account for the observed differences between the current study and the earlier work of Köster and Moeller's.[28] In any case, longer annealing times are therefore recommended for these alloys.

6 Conclusions

The following conclusions can be drawn from the current study:

(a) Partial isothermal sections of the Cu-rich corner of the Al-Cu-Zn ternary system at 200 °C and 240 °C were plotted up to about 55 at.% Al and 86 at.% Zn.
(b) Seven phases were identified at both isothermal sections of 200 °C and 240 °C: binary (αCu), γ Cu_9Al_4, η_2 CuAl, γ Cu_5Zn_8, ζ_2 $Cu_{11}Al_9$ and ε $CuZn_4$ phases and ternary τ $Cu_5Zn_2Al_3$ and τ′ Cu_3ZnAl_4 phases. No new ternary phases were found.
(c) The γ-phase was found to exist as two distinct phases: γ Cu_9Al_4 and γ Cu_5Zn_8, and XRD, together with Rietveld analysis, which showed that they both were present in Sample A5.
(d) Although the α_2 Cu_4Al, δ Cu_8Al_5 and β CuZn phases were expected at these temperatures, they were not observed. Either these phases did not penetrate the ternary far enough to be present in the samples prepared or they did not form because the samples may not have attained thermodynamic equilibrium.
(e) The solubility ranges of Cu in τ $Cu_5Zn_2Al_3$ and Zn in τ′ Cu_3ZnAl_4 reported Köster and Moeller[28] at 200 °C did not match those of the current study.

Acknowledgments The Carnegie Corporation of New York is acknowledged for funding this work through the Africa Materials Science and Engineering Network (AMSEN). Dr U. Curle of CSIR, M. Bondunrin of Wits and E. Muhuma of Mintek are also thanked for aiding in sample preparation.

References

1. W. Huang, On the Selection of Shape Memory Alloys for Actuators, *Mater. Des.*, 2002, **23**, p 11-19
2. W.M. Huang, Z. Ding, C.C. Wang, J. Wei, Y. Zhao, and H. Purnawali, Shape Memory Materials, *Mater. Today*, 2010, **13**, p 54-61
3. G. Ghosh, J. van Humbeek, and P. Perrot, Aluminium-Copper-Zinc, Ternary Alloy Systems: Phase Diagrams, Crystallographic and Thermodynamic Data, *MSIT Landolt-Börnstein IV*, 2005, **11A**(2), p 182-205
4. J. Li, W. Zhang, L. Gao, P. Gu, K. Sha, and H. Wan, Methanol Synthesis on Cu-Zn-Al and Cu-Zn-Al-Mn Catalysts, *Appl. Catal. A*, 1997, **165**, p 411-417
5. F. Huber, H. Meland, M. Rønning, H. Venvik, and A. Holmen, Comparison of Cu-Ce-Zr and Cu-Zn-Al Mixed Oxide Catalysts for Water-Gas Shift, *Top. Catal.*, 2007, **45**, p 101-104
6. E. Martinez-Flores, J. Negrete, and G. Torres Villasenor, Structure and Properties of Zn-Al-Cu Alloy Reinforced with Alumina Particles, *Mater. Des.*, 2003, **24**, p 281-286
7. S.J. Kim, K.S. Kim, S.S. Kim, C.Y. Kang, and K. Suganuma, Characteristics of Zn-Al-Cu Alloys for High Temperature Applications, *Mater. Trans.*, 2008, **49**(7), p 1531-1536
8. J.L. Murray, The Aluminium-Copper System, *Int. Mater. Rev.*, 1985, **30**, p 211-233
9. X.J. Liu, I. Ohnuma, R. Kainuma, and K. Ishida, Phase Equilibria in the Cu-Rich Portion of the Cu-Al Binary System, *J. Alloys Compd.*, 1998, **264**, p 201-208
10. P. Riani, L. Arrighi, R. Marazza, D. Mazzone, G. Zanicchi, and R. Ferro, Ternary Rare-Earth Aluminum Systems with Copper: A Review and a Contribution to their Assessment, *J. Phase Equilib. Differ.*, 2004, **25**, p 22-52
11. N. Ponweiser, C.L. Lengauer, and K.W. Richter, Re-investigation of Phase Equilibria in the System Al-Cu and Structural Analysis of the High-Temperature Phase η_1-$Al_{1-\delta}$ Cu, *Intermetallics*, 2011, **19**, p 1737-1746
12. G.V. Raynor, *Annotated Equilibrium Diagrams*, The Institute of Metals, London, 1944
13. M. Hansen and K. Anderko, *Constitution of Binary Alloys*, McGraw-Hill Book Company, New York, 1958
14. T.B. Massalski, J.L. Murray, L.H. Bennett, and H. Baker, *Binary Alloy Phase Diagrams*, American Society for Metals, Metals Park, 1986
15. A.P. Miodownik, *Binary Alloy Phase Diagrams*, Materials Information Society, Materials Park, 1990
16. B. Predel, Cu-Zn (Copper-Zinc), *Landolt-Börnstein-Group IV Phys. Chem.*, 1994, **5**(d), p 1-11
17. A.A. Presnyakov, Y.A. Gorban, and V.V. Chervyakova, Фазовая диаграмма алюминий цинк (Phase Diagram of Aluminium-Zinc), *Zh. Fiz. Khim.*, 1963, **35**(6), p 1289-1291, in Russian
18. G.R. Goldak and J.G. Parr, A High-Temperature x-ray-Diffractometer Study of the Aluminium-Zinc System in the Region 40–75 wt% Zn, *J. Inst. Met.*, 1964, **93**, p 230-233
19. J.L. Murray, The Al-Zn (Aluminium-Zinc) System, *Bull. Alloy Phase Diagr.*, 1983, **4**(1), p 55-73
20. H. Liang and Y.A. Chang, A Thermodynamic Description for the Al-Cu-Zn System, *J. Phase Equilib.*, 1998, **19**(1), p 25-37
21. W. Köster, ber den Aufbau und die Volumenänderungen der Zink-Kupfer-Aluminium-Legierungen, III. Übersicht über den Gleichgewichts vel'lauf im System Kupfer-Aluminium-Zink (The Constitution and the Volume Changes of Zn-Cu-Al Alloys, III. Summary of the Equilibrium Relationships in the System Cu-Al-Zn), *Z. Metallkd.*, 1941, **33**, p 289-296, in German
22. H.H. Arndt and K. Moeller, Die Ternäre Phase im System Kupfer-Aluminium-Zink, II. Das Zustandsgebiet der T -Phase oberhalb 500 °C (The Ternary Phase of the Cu-Al-Zn System, II. The T-Phase Field Above 500 °C), *Z. Metallkd.*, 1960, **51**, p 656-662, in German
23. J. Miettinen, Thermodynamic Description of the Cu-Al-Zn and Cu-Sn-Zn Systems in the Copper-Rich Corner, *Calphad*, 2002, **26**(1), p 119-139
24. S.-M. Liang and R. Schmid-Fetzer, Thermodynamic Assessment of the Al-Cu-Zn System, Part III: Al-Cu-Zn Ternary System, *Calphad*, 2016, **52**, p 21-3722
25. S. Murphy, Solid-Phase Reactions in the Low-Copper Part of the Al-Cu-Zn System, *Z. Metallkd.*, 1980, **71**, p 96-102

26. H. Chen, X. Xin, D.Y. Dong, Y.P. Ren, and S.M. Hao, Study on the Stability of the T′ phase in the Al-Zn-Cu ternary System, *Acta Metall. Sin.*, 2004, **17**(3), p 269-273
27. J.D. Villegas-Cardenas, M.L. Saucedo-Muñoz, V.M. Lopez-Hirata, H.J. Dorantes-Rosales, and J.L. Gonzalez-Velazquez, Effect of Phase Transformations on Hardness in Zn-Al-Cu Alloys, *Mater. Res.*, 2014, **17**(5), p 1137-1144
28. W. Köster and K. Moeller, ber den Aufbau und die Volumenänderungen der Zink-Kupfer-Aluminium-Legierungen, V. Die Aufspaltung der ternären Kristallart bei tiefen Temperaturen (The Constitution and Volume Changes of Zn-Cu-Al Alloys, V. The Division of the Ternary Phases at Low Temperatures), *Z. Metallkd.*, 1942, **34**, p 206-207, in German
29. E. Gebhardt, ber den Aufbau und die Volumenänderungen der Zink-Kupfer-Aluminium-Legierungen, VI. Übersicht über den Gleichgewichts verlauf auf der Zink-Aluminium-Seite unterhalb 350 °C (The Constitution and the Volume Changes of Zn-Cu-Al Alloys, VI. Survey of the Equilibrium Relationships on the Zn-Al Side Under 350 °C), *Z. Metallkd.*, 1942, **34**, p 208-215, in German
30. O. Bauer and M. Hansen, Der Einfluß von-dritten Metallen auf die Konstitution der Messinglegierungen, IV. Der Einfluß von Aluminium (The Effect of Third Metal on the Constitution of Brass Alloy, IV. The Effect of Al/A Constitution on the Ternary System Cu-Zn), *Z. Metallkd.*, 1932, **24**, p 1-6, in German
31. H.H. Arndt and K. Moeller, Die ternäre Phase im System Kupfer-Aluminium-Zink, I. Der Zerfall der T-Phase zwischen 200 und 300 °C (The Ternary Phase of the Cu-Al-Zn System, I. The Decomposition of the T-Phase at 200–300 °C), *Z. Metallkd.*, 1960, **51**, p 596-600, in German
32. W. Köster and K. Moeller, Über den Aufbau und die Volumenänderungen der Zink-Kupfer-Aluminium-Legierungen, II. Der Zusammenhang von CuAI, mit der ternären Kristallart (The Constitution and the Volume Changes of Zn-Cu-Al Alloys, II. The Relation of CuAl with the Ternary Phase), *Z. Metallkd.*, 1941, **33**, p 284-288, in German
33. N.E. Kandaurov, T.B. Begimov, A.A. Presnyakov, V.D. Melikhov, and Z.A. Ashirimbetov, исследование строения сплавов γ-области системымедь-алюминий-цинкпри Комнатнои температура (Structure of Alloys in the γ-Region of the Copper-Aluminum-Zinc System at Room Temperature), *Prikl. Teor. Fiz.*, 1972, **3**, p 269-275, in Russian
34. Z.A. Ashirimbetov, N.E. Kandaurov, M.M. Kalina, V.D. Melikhov, and A.A. Presnyakov, строение и свойства твердых растворов γ-области системымедь-алюминий-цинк (Structure and Properties of Solid Solutions of the γ-Region of the Cu-Al-Zn System), *Prikl. Teor. Fiz.*, 1973, **5**, p 210-213, in Russian